Available online at www.sciencedirect.com
ScienceDirect
Journal of the European Ceramic Society 29 (2009) 1393–1401
www.elsevier.com/locate/jeurceramsoc

Hydrolysis-induced aqueous gelcasting for near-net shape forming of ZTA ceramic composites

Ibram Ganesh [a,b], Susana M. Olhero [b], Paula M.C. Torres [b], Fernando J. Alves [c], José M.F. Ferreira [b,*]

[a] *Centre for Advanced Ceramics, International Advanced Research Centre for Powder Metallurgy and New Materials (ARCI), Hyderabad 500005, Andra Pradesh, India*
[b] *Department of Ceramics and Glass Engineering, CICECO, University of Aveiro, Aveiro P-3810193, Portugal*
[c] *Department of Mechanical Engineering and Industrial Management, FEUP, University of Porto, Porto, Portugal*

Received 26 April 2008; received in revised form 19 August 2008; accepted 28 August 2008
Available online 15 October 2008

Abstract

A new near-net shape forming process called "hydrolysis-induced aqueous gelcasting" (GCHAS) is reported in this paper for the consolidation of ZTA composites, ZTA-30 (70 wt.% Al_2O_3 + 30 wt.% ZrO_2) and ZTA-60 (40 wt.% Al_2O_3 + 60 wt.% ZrO_2). For comparison purposes, ceramics having the same chemical compositions were also consolidated by hydrolysis-assisted solidification (HAS). All the starting suspensions contained a solids loading of 50 vol.%. In the precursor powder mixtures, 1–5 wt.% of Al_2O_3 was replaced by equivalent amounts of AlN to enhance or promote or co-promote the consolidation of suspensions by HAS or by GCHAS, respectively. The suspensions for GCHAS were prepared by dispersing the ZTA powder precursor mixtures in a premix solution of 20 wt.% MAM (methacrylamide), MBAM (methylenebisacrylamide) and NVP (*n*-vinylpyrrolidinone) in 3:1:3 ratio in de-ionized water. Ceramics consolidated *via* GCHAS exhibited superior mechanical properties after consolidation and after sintering for 1 h at 1600 °C in comparison to those consolidated by HAS.

Keywords: ZTA ceramics; Hydrolysis-assisted solidification; Hydrolysis-induced aqueous gelcasting; Hardness; Flexural strength; Fracture toughness

1. Introduction

Zirconia-toughened alumina (ZTA) ceramics are considered as promising candidate materials for orthopaedic applications, since they offer a higher crack resistance than alumina and zirconia monoliths. Typical other applications of ZTA ceramics include pump components, bearings, bushings, cutting tool inserts, valve seats, and wear components. These ceramics are produced by die pressing of alumina and zirconia powder mixtures and then by sintering at elevated temperatures (~1600 °C). These sintered ceramics are then machined to obtain the desired shapes.[1–8] However, this die pressing route was found to be quite expensive and laborious particularly for fabricating complex-shaped products. Recently, several colloidal shaping techniques have been developed to fabricate different types of ceramic components with near-net shape.[9–14] Net shaping of ceramics is of great importance because post-sintering machining operations can be minimized or eliminated thereby saving a lot of time and money.[15] This is extremely important particularly in the case of mass productions of several advanced ceramics where high productivity with minimum cost must be fulfilled.[10–15] Therefore, the selection of the forming technique has direct impacts on the productivity and on the ultimate quality and the cost of the manufactured products. Moreover, colloidal approaches also enable high green density and excellent chemical homogeneity to be achieved in the consolidated bodies.

Among the various existing near-net shape forming methods, hydrolysis-assisted solidification (HAS) was found to be the most simple and inexpensive technique that has been used to consolidate several kinds of ceramics in which alumina was a minor or major constituent.[11,12] In this process, the consolidation of suspensions takes place due to the hydrolysis of AlN powder ($AlN + 3H_2O \rightarrow Al(OH)_3 + NH_3$), which causes drastic changes in the viscosity of the suspension leading to

* Corresponding author. Tel.: +351 234 370242; fax: +351 234 370204.
E-mail address: jmf@ua.pt (J.M.F. Ferreira).

0955-2219/$ – see front matter © 2008 Elsevier Ltd. All rights reserved.
doi:10.1016/j.jeurceramsoc.2008.08.033

Table 1
Precursor powder mixtures used for the preparation of ZTA-30 and ZTA-60 ceramics by the two colloidal processing routes

Sample[a]	Processing route	Slurry medium	Al_2O_3 (wt.%)	ZrO_2 (wt.%)	AlN (wt.%)
30HAS-1	HAS	Water	49.12	30.05	0.82
30HAS-2	HAS	Water	68.26	30.11	1.61
30HAS-3	HAS	Water	67.39	30.18	2.42
30HAS-4	HAS	Water	66.52	30.23	3.24
30HAS-5	HAS	Water	65.98	29.99	4.02
30GCHAS-1	GCHAS	Premix solution	49.12	30.05	0.82
30GCHAS-2	GCHAS	Premix solution	68.26	30.11	1.61
30GCHAS-3	GCHAS	Premix solution	67.39	30.18	2.42
30GCHAS-4	GCHAS	Premix solution	66.52	30.23	3.24
30GCHAS-5	GCHAS	Premix solution	65.98	29.99	4.02
60HAS-5	HAS	Water	38.03	60.35	1.62
60GCHAS-5	GCHAS	Premix solution	38.03	60.35	1.62

[a] All the suspensions contained 50 vol.% solids. The numbers 30 and 60 in the sample codes stand for the wt.% of zirconia concentration in the samples. GCHAS and HAS stand for "hydrolysis-induced aqueous gelcasting" and "hydrolysis-assisted solidification" processes, respectively. The numbers 1–5 represent the wt.% of Al_2O_3 that was replaced by an equivalent amount of AlN.

consolidation. The aluminium hydroxide formed due to AlN hydrolysis acts as cement and grants high stiffness to the consolidated parts, which in turn helps in keeping the shape of the part intact during subsequent processing steps such as drying and binder removal, thereby minimizing the post-sintering machining operation.[12] Furthermore, as the formation of the green body is not affected by an externally applied pressure or water absorption by an absorptive mould, this process effectively utilizes various thermally activated chemical processes *in situ*. However, as the parts consolidated by HAS are brittle and exhibit relatively poor strength, certain components like crucibles, bushings, valve seats, pump components, etc., having thin wall and complex shapes are difficult to fabricate.[12]

In contrast to HAS process, aqueous gelcasting (GC) offers the same near-net shape forming features while conferring high strength to the as consolidated parts.[9,13–15] Furthermore, the gelcast consolidates can be green machined to obtain desired dimensions. In spite of these advantages, the major drawback of gelcasting is associated to the drying step of the consolidated parts, especially when they have different thickness at different places. The thermal/moisture gradients generated during drying lead to appearance of cracks in the consolidated parts.[13–15]

This paper reports on a new near-net shaping technique, "hydrolysis-induced aqueous gelcasting" (GCHAS),[16] which is a combination of the HAS and gelcasting (GC) processes aiming at addressing the problems associated to the drying step of consolidates formed by gelcasting. The synergetic effect of these two processes confers exceptionally high strength to the as consolidated parts and facilitates uniform drying of consolidates, as water is partially consumed upon hydrolysis of AlN. The concomitant increase in pH of the system can also favourably change the permeability of the green bodies and minimize the thermal/moisture gradients. Two ZTA composites (ZTA-30, 70 wt.% Al_2O_3 + 30 wt.% ZrO_2 and ZTA-60, 40 wt.% Al_2O_3 + 60 wt.% ZrO_2) were consolidated by GCHAS and HAS from aqueous suspensions containing 50 vol.% solids. In our previous study,[12] dense β-$Si_4Al_2O_2N_6$ ceramics with absence of open porosity were obtained after sintering (1675 °C, 4 h) green bodies consolidated by HAS from aqueous suspensions containing 50 vol.% solids in which 5 wt.% of Al_2O_3 was replaced in the precursor powder mixture by an equivalent amount of AlN. The replacement of higher percentages of alumina by equivalent amounts of AlN led to sintered ceramics with a lot of open porosity. Based on this information, the maximum replacement of Al_2O_3 by AlN was limited to 5 wt.% in the present work. The physical and mechanical properties of sintered (1600 °C, 1 h) ZTA ceramics were evaluated through different techniques and the influence of processing routes on their final properties is discussed.

2. Experimental procedure

2.1. Powder processing

An alumina powder (CT-3000SG, Alcoa-Chemie GmbH, Germany, with an average particle size, D_{50} = 0.8 μm) and a zirconia powder (Tosoh-Zirconia, TZ-3YS, Yamaguchi, Japan, D_{50} = 0.43 μm) were used along the present work as the main components. A high purity AlN powder (Grade C, H.C. Stark, Germany, D_{50} = 0.33 μm, oxygen content <1.3%) was also used as consolidating agent.

The precursor compositions used for the preparation of ZTA-30 (70 wt.% Al_2O_3 + 30 wt.% ZrO_2) and ZTA-60 (40 wt.% Al_2O_3 + 60 wt.% ZrO_2) ceramics following HAS and GCHAS route are summarized in Table 1. The numbers 30 and 60 in the sample codes indicate the wt.% of zirconia in the composite. The remaining of the sample codes stands for the consolidation process: HAS and GCHAS. For both consolidation techniques, 1–5 wt.% Al_2O_3 was replaced in the precursor powder mixtures by equivalent amounts of AlN as consolidating agent.

All the suspensions were prepared with 50 vol.% solids by wet ball milling for 24 h in polypropylene bottles using alumina balls (the charge to balls ratio was 1:3). For the HAS process, an aqueous Dolapix CE 64 (Zschimmer and Schwarz, Germany) solution, at the ratio of 0.7 wt.% on the powder weight basis, was used as dispersing medium. The as obtained homogenous suspensions were filtered off and degassed for 5 min by vacuum pumping. To the same degassed suspension, the required amount of AlN was added and mixed for further 2 h under

the same ball milling conditions to obtain the suspensions for HAS, which were poured into split type aluminium moulds (60 mm × 30 mm × 30 mm) for consolidation.

The suspensions for GCHAS were prepared by dispersing the ZTA powder precursor mixtures (Table 1) in an organic premix solution[13,14] obtained by dissolving 20 wt.% MAM (methacrylamide), MBAM (methylenebisacrylamide) and NVP (*n*-vinylpyrrolidinone) in 3:1:3 ratio in de-ionized water in the presence of the same dispersing agent (Dolapix CE 64, 0.7 wt.% on the powder weight basis). De-agglomeration was performed for 24 h in polypropylene bottles containing alumina balls (12 mm diameter) using a roller mill. The weight ratio between powder and balls was of 1:3. The homogenous suspensions thus obtained were filtered off and degassed for 5 min by vacuum pumping. To all the homogeneous suspensions, 1-octanol at the ratio of 1 μL/g of suspension was added as de-airing agent. After introducing a polymerization initiator (10 wt.% aqueous solution of ammonium per-sulphate, APS) and a catalyst (tetramethylethylenediammine, TEMED) at the ratio of 4 and 2 μL/g of suspension, respectively,[13,14] the homogenized suspensions were once again degassed for 2 min prior to casting in non-porous white petroleum jelly coated split-type aluminium moulds (60 mm × 30 mm × 30 mm).[13,14] The completion of the gelling/setting process was then allowed to occur under ambient conditions. The consolidated parts were dried under controlled conditions (90 °C for 24 h, 90% relative humidity) to avoid cracking and non-uniform shrinkage due to rapid drying after de-moulding. The ZTA samples consolidated by HAS and GCHAS were heat treated at a rate of 1 °C/min up to 500 °C and held at this temperature for 2 h. The sintering was then conducted at a heating rate of 5 °C/min up to 1600 °C with 1 h holding time at this temperature.

2.2. Characterization techniques

Particle size analysis of the powders was performed by using light scattering equipment (Coulter LS 230, UK, Fraunhofer optical model). The viscosity of slurries was measured using a rotational Rheometer (Bohlin C-VOR Instruments, Worcestershire, UK). The measuring configuration adopted was a cone and plate (4°, 40 mm, and gap of 150 μm), and flow measurements were conducted between 0.1 and 800 s^{-1}. The same configuration was used to obtain information about the gelation behaviour and the evolution of gel stiffness under dynamic measurements of G' and G'' in the linear viscoelastic region. A time sweep was conducted for 30 min at a constant frequency of 1 Hz. A frequency sweep from 1 to 100 Hz under a constant stress of 100 Pa was performed immediately after 30 min of gel time, i.e., the time corresponding to the crossover point of the G' and G'' curves.

Bulk density (BD), apparent porosity (AP), and water absorption (WA) capacity of the sintered ZTA ceramics were measured in aqueous media according to Archimedes principle (ASTM C372) using a Mettler balance (AG 245, Mettler Toledo, Switzerland). At least, three density measurements were averaged for each sample (±0.01 error).[16,17] XRD patterns were recorded on a Rigaku (Tokyo, Japan) using diffracted beam mono-chromated Cu Kα (0.15406 nm) radiation source.[18] Crystalline phases were identified by comparison with PDF-4 reference data from International Centre for Diffraction Data (ICDD).[19] Microstructures of dense ZTA ceramics were examined by SEM (Hitachi S-4100, Tokyo, Japan) on thermally etched (1500 °C for 10 min) surfaces after coating with carbon for conductivity. The mechanical properties evaluated were hardness (H), fracture toughness (K_{Ic}) and flexural strength. Hardness was determined by applying a Vickers indenter and calculated as $H = P/2d^2$, d being the half-diagonal indentation impression and P the indentation load (10 kg). The flexural strength was measured using the 3-point bend test (JIS-R1601). Further, the fracture toughness value (K_{Ic}) was calculated on the basis of the indentation method [$K_{Ic} = Ha^{1/2} \times 0.203(C/a)^{-3/2}$].[20] Here, $2a$ represents Vickers indent diagonal length, $2C$ the resultant crack length and H is the Vickers hardness (H_V = kg/mm^2 = 10 MPa). While measuring fracture toughness, five to six samples were examined per case; in order to check the reproducibility of results and all the five readings were averaged out.[13,14] The required hardness, crack and diagonal length data was collected using a microhardness tester (Leitz Wetzler, Germany) by holding the indenter tip (with 137°) under 10 kg load for 20 s on the polished to mirror finish surface of the sample.

3. Results and discussion

3.1. Characteristics of the suspensions

The viscosity *versus* shear rate curves of the HAS (30HAS-1 to 30HAS-5) and GCHAS (30GCHAS-1 to 30GCHAS-5) suspensions (see Table 1) are presented in Figs. 1 and 2, respectively. The HAS suspensions exhibit a shear thinning behaviour throughout the whole γ range, with a first abrupt decrease of viscosity followed by a much less accentuated decreasing trend. The abrupt change in viscosity within the low shear rate range is also a common feature to the GCHAS suspensions, followed by a near-Newtonian plateau between 150 and 350 s^{-1} and ending with an apparent shear thickening trend for $\gamma > 350\ s^{-1}$. Nor-

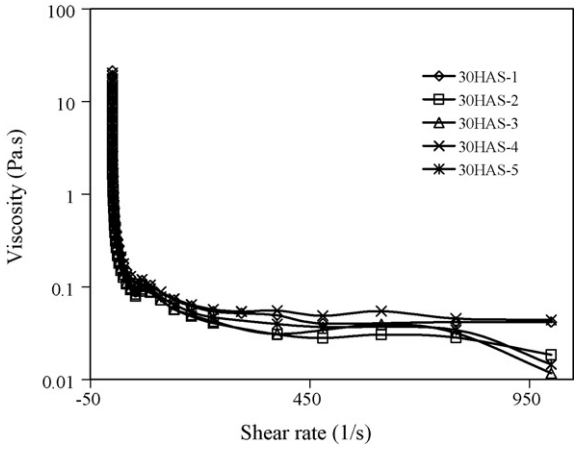

Fig. 1. Viscosity *versus* shear rate of aqueous suspensions containing 50 vol.% ZTA-30 precursor mixture in which 1–5 wt.% Al_2O_3 was replaced by an equivalent amount of AlN.

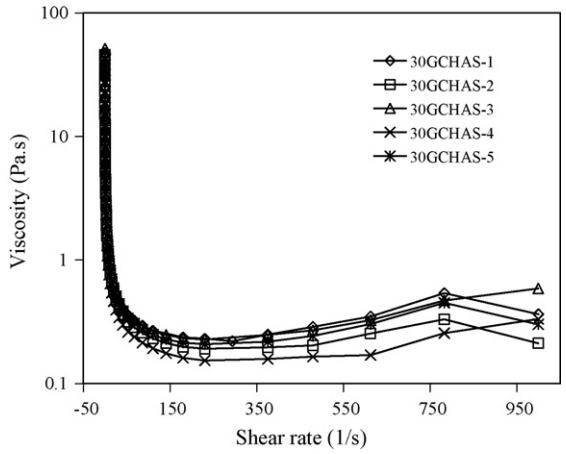

Fig. 2. Viscosity *versus* shear rate of aqueous–organic gelcast premix suspensions containing 50 vol.% ZTA-30 precursor powder mixture, in which 1–5 wt.% Al_2O_3 was replaced by an equivalent amount of AlN.

mally, the presence of coarse particles or agglomerates or both is responsible for the shear thickening behaviour.[21] These results suggest that a better degree of de-agglomeration was achieved in the HAS suspensions upon ball milling in comparison to GCHAS systems. The latter suspensions contain always some amounts of un-dissolved MBAM particles because of its low solubility in water (only 2 wt.%),[9,14,15] which were not filtered (mesh size <75 μm) away prior to dispersing ceramic powders. In any case, the filter will hardly retain all the un-dissolved MBAM particles that can cause shear thickening of GCHAS suspensions. Furthermore, the GCHAS suspensions exhibit viscosity values that are three to four times higher than those of HAS suspensions. It can also be seen from Figs. 1 and 2 that the addition of AlN did not cause significant or systematic changes in suspension's viscosity.[22,23]

The comparison of the flow behaviour of 60HAS-5 and 60GCHAS-5 suspensions in Fig. 3 over a shear rate range of 0–750 s^{-1} does not show any significant difference in these zirconia richer compositions, probably due to the fineness of this powder ($D_{50} = 0.43$ μm *versus* $D_{50} = 0.8$ μm for alumina).

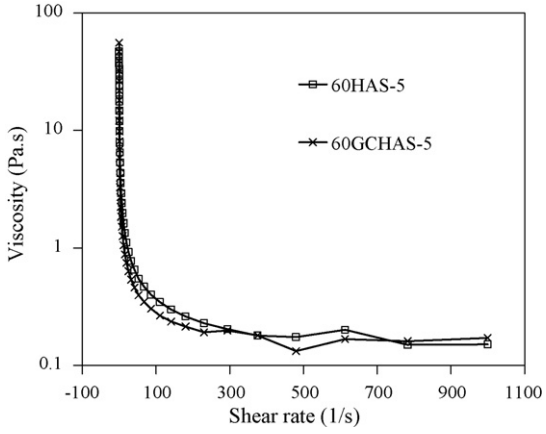

Fig. 3. Comparison of the flow behaviours of de-agglomerated suspension containing 50 vol.% of ZTA-60 precursor mixtures dispersed in water (60HAS-5) and in the aqueous–organic gelcast premix solution (60GCHAS-5).

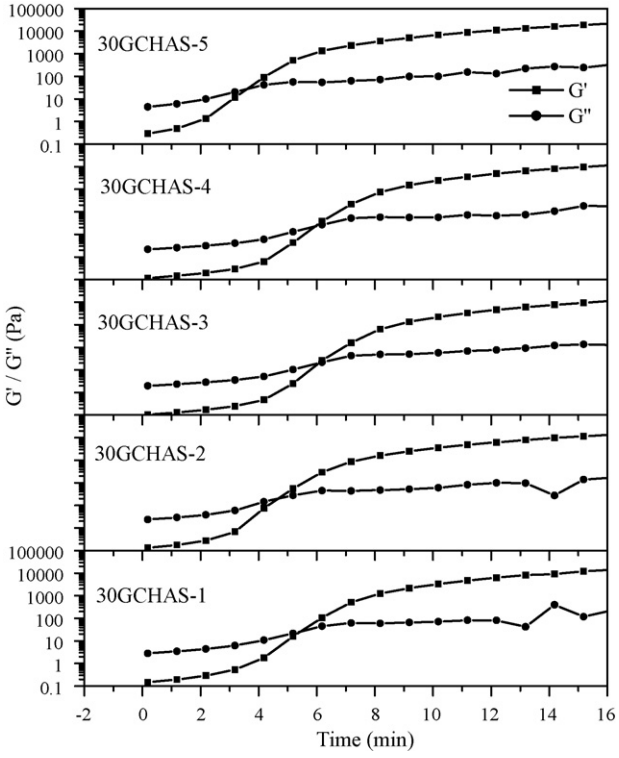

Fig. 4. Combined effects of free radical polymerization of organic monomers and AlN hydrolysis on the setting behaviour of suspensions containing 50 vol.% ZTA-30 precursor mixtures in which 1–5 wt.% Al_2O_3 was replaced by equivalent amounts of AlN.

Specific interactions between the processing additives and the surface of the two different powders can also account for absence of shear thickening effects in comparison to Fig. 2, making them suitable for casting processes.

The evolution of the internal structure of the GCHAS-1 to GCHAS-5 suspensions upon addition of polymerization initiator (APS) and catalyst (TEMED) is presented in Fig. 4 as a function of reaction time. Both the storage modulus or elastic component (G') and the loss modulus or viscous component (G'') increase with time increasing. The viscous character predominates over the elastic one throughout the first period that starts with the addition of polymerization initiator and ends at the crossover point where $G' = G''$. The elapsed time up to this point is usually taken as the gelation time, above which the elastic character of the gelling systems predominates over the viscous one ($G' > G''$) by values that can go beyond one to two orders of magnitude.

The mechanical spectra of the systems 30GCHAS-1 to 30GCHAS-5 recorded at ambient temperature immediately after the crossover point are presented in Fig. 5. Due to the great differences in magnitude between G' and G'', the dynamic analysis was restricted to the elastic component only. In fact, under the tested conditions, the measurement of G'' is no longer reliable because it depends on the instrumental resolution of the phase lag between sinusoidal stress and strain.[21] Fig. 5 shows that all the curves run almost parallel to the *x*-axis, a characteristic behaviour of stiff gels. Furthermore, G' is enhanced over the whole frequency range tested with increasing added amounts of AlN. It has been reported that AlN causes a reduc-

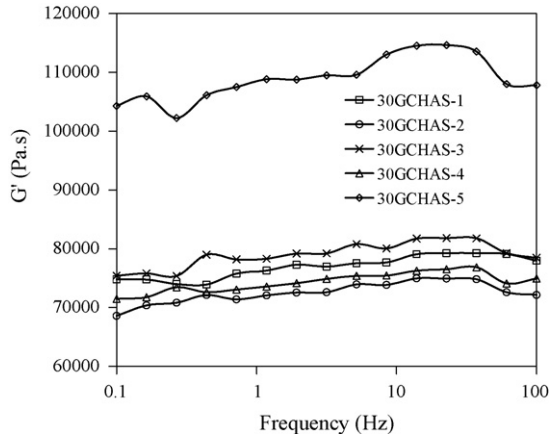

Fig. 5. Mechanical spectra measured immediately after the gelation time (crossover point of G' and G'') for consolidates derived from 50 vol.% ZTA-30 precursor mixtures, in which 1–5 wt.% Al_2O_3 was replaced by equivalent amounts of AlN, dispersed in the aqueous–organic premix solution.

tion in liquid component and an increase in solid component of the suspension.[22,23] Gelling particulate systems exhibit varying visco-elastic characteristics with the elastic component (the gel strength) usually increasing with time. The specific behaviour observed also depends on other experimental conditions such as solids loading, the concentration of processing additives and temperature. The data presented in Fig. 5 suggest that under the experimental conditions used in the present work, the high strength gels can be formed from 50 vol.% solids loading suspensions of ZTA-30 precursor mixtures in which ≥3 wt.% Al_2O_3 has been replaced by equivalent amounts of AlN.

3.2. Characteristics of green consolidates

Table 2 lists the values of viscosity of suspensions (at $\gamma = 140\,s^{-1}$), the amount of NH_3 to be released upon complete hydrolysis of AlN, the setting time of suspensions, as well as the values of green density, green porosity, percentage of linear shrinkage upon drying and green strength of consolidates. In general, GCHAS suspensions exhibit higher viscosity values in comparison to HAS suspensions. Furthermore, the viscosity of the HAS suspensions slightly increased with increasing concentrations of AlN, whereas a less clear trend is apparent in the case of GCHAS suspensions. Usually, AlN undergoes the following three reactions (Eqs. (1)–(3)) in the presence of water:

$$AlN + 2H_2O \rightarrow AlO(OH) + NH_3 \quad (1)$$

$$NH_3 + H_2O \rightarrow NH_4OH \quad (2)$$

$$AlO(OH) + H_2O \rightarrow Al(OH)_3 \quad (3)$$

It consumes water, releases ammonia, and forms aluminium hydroxides. All these events contribute to an increase of the viscosity of the suspensions. According to data in Table 2, the highest amount of NH_3 gas (1.66 wt.%) is released by the precursor mixtures 30GCHAS-5 and 30HAS-5 containing 4.02 wt.% AlN. This released amount is well within the solubility limit of ammonia in water (at 20 °C, 31.34 mol NH_3/L of water at STP, or ~532 g of NH_3 in 1000 g water). Therefore, the formation of gas bubbles that can be entrapped in the suspensions and in the green consolidates is not expected to occur in a great extent under the present used conditions.[12] But the consequent increase in the suspensions pH towards the isoelectric point of alumina, in conjunction with the other products of reactions (1)–(3) will tend to increase the viscosity of the suspensions. Nevertheless, all the suspensions exhibit acceptable viscosity values for casting processes within the utilizable time frame.[24]

The denser zirconia (theoretical density, $\rho_{th} = 5.89\,g/cm^3$, in comparison to that of alumina, $\rho_{th} = 3.89\,g/cm^3$) explains the higher absolute green density values of ZTA-60 bodies richer in this oxide, but the percentage of green porosity was practically unaffected by the use of different compositions. The packing ability to the GCHAS systems was not affected by the added amount of AlN, contrarily to the HAS ones that revealed a decreasing trend with increasing amounts of AlN. For

Table 2
Properties of slurries and of green ZTA-30 and ZTA-60 consolidates obtained by the two colloidal processing routes

Sample[a]	Slurry viscosity at $\gamma = 140\,s^{-1}$ (mPa s)	NH_3 due to hydrolysis of AlN (wt.%)	Setting time (min)	Green density (g/cm^3)	Green porosity[b] (%)	Linear shrinkage upon drying (%)	Green strength (MPa)
30HAS-1	72.5	0.340	<2880	2.77 ± 0.03	39.16	2.088 ± 0.33	2.2 ± 1.01
30HAS-2	71.9	0.667	<2880	2.42 ± 0.02	46.85	1.968 ± 0.37	2.93 ± 0.96
30HAS-3	72.8	1.003	<1440	2.36 ± 0.04	48.17	2.318 ± 0.15	4.04 ± 1.23
30HAS-4	74.6	1.343	<1440	2.57 ± 0.16	43.55	1.968 ± 0.43	4.09 ± 2.10
30HAS-5	78.3	1.666	<1440	2.40 ± 0.06	47.29	1.582 ± 0.20	7.76 ± 2.34
30GCHAS-1	269	0.340	5.64	2.42 ± 0.08	46.85	2.154 ± 0.07	9.79 ± 1.16
30GCHAS-2	231	0.667	4.72	2.56 ± 0.11	43.77	2.089 ± 0.32	16.33 ± 2.41
30GCHAS-3	266	1.003	6.19	2.54 ± 0.08	44.21	2.137 ± 0.28	17.89 ± 2.19
30GCHAS-4	193	1.343	6.14	2.61 ± 0.14	42.68	2.237 ± 0.04	18.19 ± 2.43
30GCHAS-5	249	1.666	3.46	2.47 ± 0.02	45.75	1.623 ± 0.15	20.03 ± 2.31
60HAS-5	346	0.671	<1440	2.841 ± 0.42	44.58	1.62 ± 0.31	5.35 ± 0.76
60GCHAS-5	273	0.671	4.2	2.845 ± 0.32	44.50	1.642 ± 0.14	20.47 ± 2.49

[a] All the suspensions contained 50 vol.% solids. The numbers 30 and 60 in the sample codes stand for the wt.% of zirconia concentration in the samples. GCHAS and HAS stand for "hydrolysis-induced aqueous gelcasting" and "hydrolysis-assisted solidification" processes, respectively. The numbers 1–5 represent the wt.% of Al_2O_3 that was replaced by an equivalent amount of AlN.

[b] The percentage of theoretical density (ρ_{th}) values of ZTA-30 ($4.553\,g/cm^3$) and ZTA-60 ($5.126\,g/cm^3$) were calculated based on the rule of mixture of alumina ($\rho_{th} = 3.98\,g/cm^3$) and zirconia ($\rho_{th} = 5.89\,g/cm^3$) theoretical densities. The percentage of green porosity is given by ($100 - \%\rho_{th}$).

Table 3
Properties of sintered (1600 °C, 1 h) ZTA-30 and ZTA-60 ceramics consolidated by the two colloidal processing routes

Sample[a]	Bulk density[b] (g/cm^3)	Theoretical density (%)	Apparent porosity (%)	Water absorption (%)	Total linear shrinkage (%)	Hardness, H_V (kg/mm^2)	Fracture toughness ($MPa\,m^{1/2}$)	Flexural strength (MPa)
30HAS-5	4.01	88.07	0.9	0.79	20.766 ± 0.60	1315.5 ± 29	4.86 ± 0.48	463.54 ± 16.6
30GCHAS-5	4.17	91.59	0.2	0.04	21.090 ± 0.76	1446.5 ± 31	5.48 ± 0.45	610.0 ± 36.44
60HAS-5	4.65	90.71	0.01	0.02	18.722 ± 0.41	1293.6 ± 39	5.65 ± 0.91	483.0 ± 37.42
60GCHAS-5	4.92	95.98	0.10	0.02	19.084 ± 0.18	1330.3 ± 16	7.38 ± 0.38	660.52 ± 33.2

[a] All the suspensions contained 50 vol.% solids. The numbers 30 and 60 in the sample codes stand for the wt.% of zirconia concentration in the samples. GCHAS and HAS stand for "hydrolysis-induced aqueous gelcasting" and "hydrolysis-assisted solidification" processes, respectively. The numbers 1–5 represent the wt.% of Al_2O_3 that was replaced by an equivalent amount of AlN.

[b] The percentage of theoretical density (ρ_{th}) values of ZTA-30 (4.553 g/cm^3) and ZTA-60 (5.126 g/cm^3) were calculated based on the rule of mixture of alumina (ρ_{th} = 3.98 g/cm^3) and zirconia (ρ_{th} = 5.89 g/cm^3) theoretical densities. The percentage of green porosity is given by $(100 - \%\rho_{th})$.

the 60HAS-5 and 60GCHAS-5 systems similar packing densities were obtained. Upon drying, the GCHAS consolidates shrunk more in comparison to the HAS ones. This difference is consistent with a more intricate 3D network of fine pores derived from the polymerization reactions upon gelcasting. The higher capillary pressures developed in these finer pores is responsible for the higher sensitivity of gelcast bodies to drying,[13–15] which are equivalent to a higher external pressure applied to consolidates during this processing step. Contrarily, the setting by HAS involves a coagulation mechanism promoted by the shift of pH towards the isoelectric point of alumina, which is prone to generate a more open pore structure in which lower magnitude capillary forces will develop upon drying, explaining the lower observed values of linear shrinkage. Interestingly, all consolidates exhibit linear shrinkage values upon drying <3%, which was considered the safety range for a successful fabrication of complex-shaped ceramic components with near-net shape by gelcasting.[15,16,24] This obviously requires the use of suspensions with a fairly high solids content.

Green strength data in Table 2 show that the GCHAS consolidates are stronger than the HAS ones. This seems quite obvious considering that both strengthening mechanisms (i) polymerization of organic MAM, NVP and MBAM monomers and, (ii) the cementing action of $Al(OH)_3$ formed by AlN hydrolysis, will be active in the GCHAS consolidates, whereas only the last one will be involved in the case of HAS process. It can also be noted that the green strength of HAS consolidates increased with increasing added amounts of AlN. The boehmite formed due to AlN hydrolysis connects the ceramic particles into a stiff body[11,34,35] and the amount of boehmite formed increases with the AlN concentration in the suspension. Furthermore, the green strength seems to be least influenced by the overall chemical composition since the 30GCHAS-5 and 60GCHAS-5 consolidates exhibit comparable strength values, of 20.03 ± 2.31 and 20.47 ± 2.49 MPa, respectively (Table 2). These results suggest that GCHAS is an interesting new processing route for consolidating high strength ZTA ceramics with near-net shape. In fact, these are the highest values ever reported for ZTA ceramics.[1–7] A green body with about 20 MPa can be machined to obtain desired dimensions which will minimize the expensive post-sintering machining operation.

3.3. Characteristics of sintered bodies

The values of bulk density, apparent porosity, water absorption capacity, hardness, fracture toughness, and flexural strength of ZTA-30 and ZTA-60 ceramics sintered for 1 h at 1600 °C are presented in Table 3 together with the percentage of total linear shrinkage. The ZTA-30 samples exhibit bulk density values in the range of 4.01–4.23 g/cm^3, whereas those of ZTA-60 samples varied in the range of 4.65–4.94 g/cm^3. These differences are mostly due to the higher proportion of denser zirconia in the latter samples, which also achieved higher degrees of densification. The ZTA ceramics consolidated by GCHAS exhibit higher bulk densities in comparison to those prepared by HAS, which can be attributed to an improved homogeneity of the green bodies achieved by GCHAS. But irrespective of the preparation method and chemical composition, all the sintered samples exhibit apparent porosity and water absorption capacity values less than 0.9% and 0.8%, respectively.

The influence of added AlN replacing 1–5 wt.% equivalent amounts of Al_2O_3 to in the precursor mixture on the bulk density and percentage of linear shrinkage of ZTA-30 ceramics sintered for 1 h at 1600 °C can be seen from Fig. 6. Both properties decreased with increasing amounts of replaced alumina, suggesting the entrapment of some gas bubbles derived from the hydrolysis of AlN. The degree of densification and the shrinkage of the samples are inversely related as expected. Interestingly, all the sintered samples exhibit linear shrinkage values <22%. This means that we are in the safety range to fabricate components with near-net shape by gelcasting, which according to Janney et al.,[15,24] require total shrinkages <25%. The apparent porosity and water absorption capacity of ZTA ceramics sintered for 1 h at 1600 °C are found to be inline to their corresponding bulk density and linear shrinkage properties as can be seen from Fig. 7. It can also be seen that the sintered samples consolidated by GCHAS exhibit apparent porosity and water absorption capacity values close to zero when the amount of replaced alumina is up to 4 wt.%. But the sintered samples consolidated by HAS show apparent porosity and water absorption capacity values that reach about 0.8% and 0.9%, respectively for the highest amount of replaced alumina.

Table 3 also reveals that ZTA ceramics richer in zirconia exhibit improved fracture toughness and flexural strength and

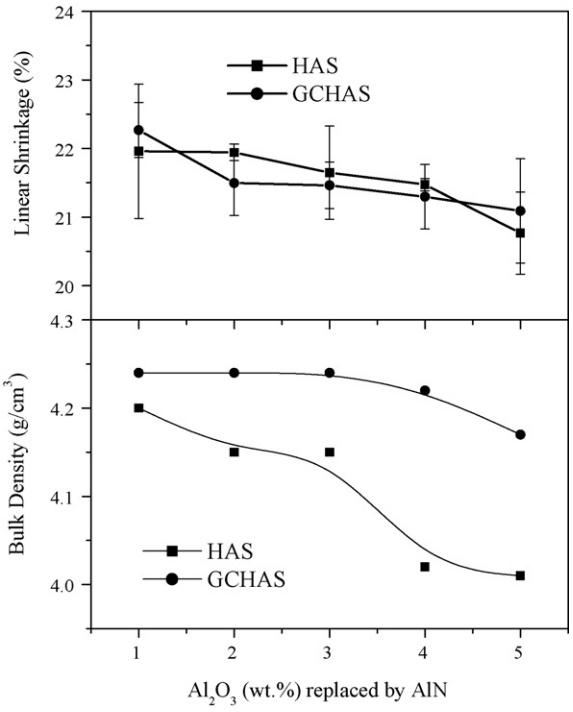

Fig. 6. Evolution of bulk density and linear shrinkage of ZTA-30 ceramics consolidated by HAS and GCHAS from slurries containing 50 vol.% solids and sintered for 1 h at 1600 °C as a function of alumina contents (1–5 wt.%) replaced by equivalent amounts of AlN.

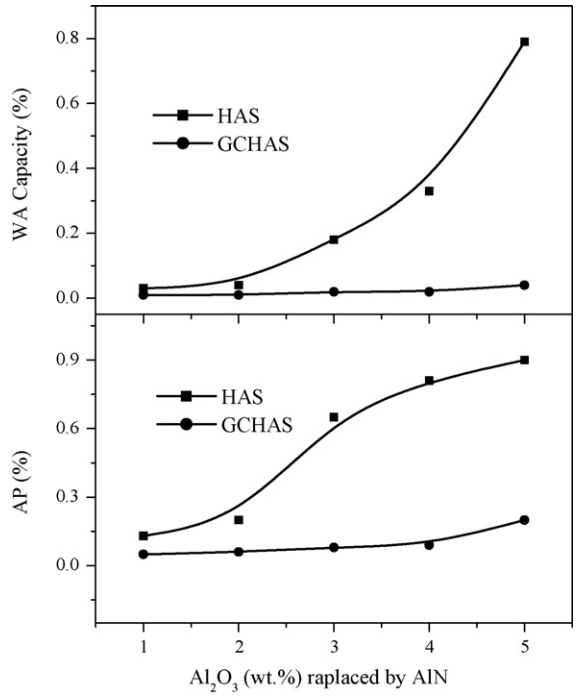

Fig. 7. Evolution of apparent porosity and water absorption capacity values of ZTA-30 ceramics consolidated by HAS and GCHAS from slurries containing 50 vol.% solids and sintered for 1 h at 1600 °C as a function of alumina contents (1–5 wt.%) replaced by equivalent amounts of AlN.

lower hardness values, as expected. Concerning the influence of the consolidation method, the higher fracture toughness and 3-point bend strength values measured for the GCHAS samples and the close relationship between these mechanical properties and bulk density, enable to point out hydrolysis-induced aqueous gelcasting as being more reliable. The overall mechanical properties measured for the ZTA ceramics are comparable to those reported for similar materials in the literature.[1–8,25] The

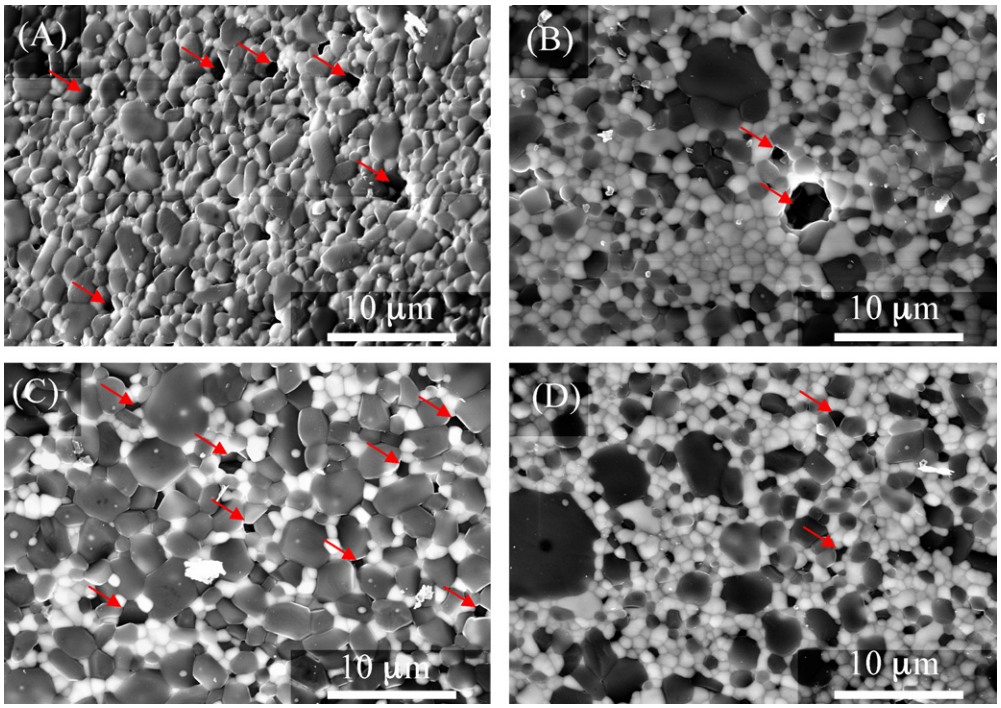

Fig. 8. SEM micrographs of sintered (1600 °C, 1 h) ceramics: (A) 30HAS-5; (B) 60HAS-5; (C) 30GCHAS-5; and (D) 60GCHAS-5. The arrows indicate small pores, which are more frequent in the ZTA-30 ceramics.

toughening mechanisms operating in ZTA ceramics are due to t → m phase transformation of zirconia, which occurs with a volume expansion and an associated shear strain, resulting in compressive stresses that reduce propagation.[1–8,25] This necessitates extra work for further crack propagation. Cracks deflected by localized stress fields and the formation of micro-cracks able to absorb the fracture energy will also account for the increased material toughness.

The differences in mechanical properties between the 30HAS-5 and 30GCHAS-5 ceramics are certainly related to different microstructural features, as shown in Fig. 8. The whiter areas observed in the SEM microstructures are due to zirconia, explaining the larger white fraction presented by ZTA-60 ceramics. A close look into these micrographs reveals that ceramics consolidated by HAS are apparently more porous than those consolidated by GCHAS and that ZTA-30 ceramics achieved a lower densification degree than ZTA-60 ceramics, confirming the density and porosity data presented in Table 3. These microstructural features tend to confirm the expected close relationship between the degree of homogeneity of the consolidated green bodies and the densification behaviour of upon sintering. Moreover, besides alumina and zirconia, no other phases could be seen at the grain boundaries, being consistent with the XRD results of the GCHAS samples presented in Fig. 9. All the sintered bodies revealed XRD lines due only to $[(ZrO_2)_{0.91}(Y_2O_3)_{0.09}]_{0.917}$ and corundum phases. For the purpose of easy comparison, the standard XRD data reported in ICDD files for corundum (α-Al_2O_3, No.: 00-046-1212), monoclinic zirconia (m-ZrO_2, No.: 00-037-1484) and zirconia–yttria compound $\{[(ZrO_2)_{0.91}(Y_2O_3)_{0.09}]_{0.917}$, No.: 01-083-0113} are also presented in Fig. 9. These results suggest that no unhydrolyzed AlN is left over in the sintered samples.

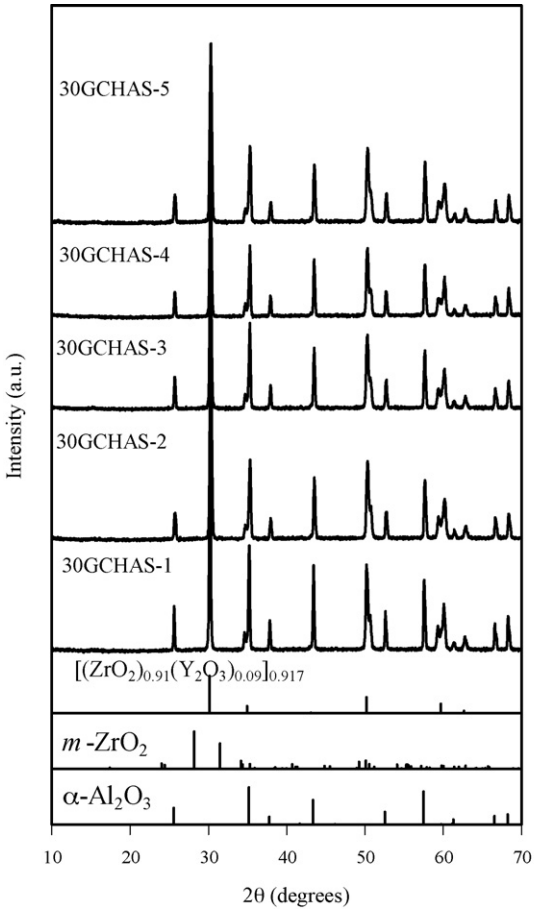

Fig. 9. XRD patterns of sintered (1600 °C, 1 h) ceramics consolidated *via* hydrolysis-induced aqueous gelcasting (GCHAS) from slurries containing 50 vol.% ZTA-30 precursor powder mixture in which 1–5 wt.% of Al_2O_3 was replaced by equivalent amounts of AlN (α-Al_2O_3, ICDD File No.: 00-046-1212; m-ZrO_2, ICDD File No.: 00-037-1484; $((ZrO_2)_{0.91}(Y_2O_3)_{0.09})_{0.917}$, ICDD File No.: 01-083-0113).

4. Conclusions

The following conclusions can be drawn from the above study:

1. Different types of dense ZTA ceramics, which have potential for orthopaedic applications, can be fabricated following colloidal processing techniques.
2. Hydrolysis-induced aqueous gelcasting is a superior processing route for consolidating high green strength ZTA ceramics (20 MPa) with near-net shape, which permits green machining in comparison to HAS or gelcasting alone. Up to 5 wt.% Al_2O_3 can be replaced in the precursor mixture by equivalent amounts of AlN to induce or promote consolidation.
3. The ceramics consolidated by GCHAS process could be dried without any difficulty irrespective of the shape and the size of the components.
4. The sintered ZTA ceramics consolidated by hydrolysis-induced aqueous gelcasting process exhibit higher fracture toughness and flexural strength in comparison to those consolidated by HAS.

Acknowledgements

IG thanks SERC-DST (Government of India) for awarded BOYSCAST fellowship (SR/BY/E-04/06). S.M. Olhero wishes to thank to Foundation for Science and Technology of Portugal for the financial support under the grant SFRH/BPD/27013/2006. The financial support of CICECO is also acknowledged.

References

1. Claussen, N., Fracture toughness of Al_2O_3 with an un-stabilized ZrO_2 dispersed phase. *J. Am. Ceram. Soc.*, 1976, **59**, 49–51.
2. Wang, J. and Stevens, R., Review—zirconia-toughened alumina (ZTA) ceramics. *J. Mater. Sci.*, 1989, **24**(10), 3421–3440.
3. Tsukuma, K., Ueda, K. and Shimada, M., Strength and fracture toughness of *iso*-statically hot-pressed composites of Al_2O_3 and $Y_2O_3^-$ partially-stabilized ZrO_2. *J. Am. Ceram. Soc.*, 1985, **68**(1), C4–C5.
4. Tsukuma, K., Takahata, T. and Shiomi, M., Strength and fracture toughness of Y-TZP, Ce-TZP, Y-TZP/Al_2O_3, and Ce-TZP/Al_2O_3. *Advanced in Ceramics, vol. 24: Science and Technology of Zirconia III*. The American Ceramic Society, Columbus, OH, 1988, pp. 721–728.
5. Tuan, W. H., Chen, R. Z., Wang, T. C., Cheng, C. H. and Kuo, P. S., Mechanical properties of Al_2O_3/ZrO_2 composites. *J. Eur. Ceram. Soc.*, 2002, **22**(16), 2827–2833.

6. Shin, Y., Rhee, Y. and Kang, S., Experimental evaluation of toughening mechanism in alumina–zirconia composites. *J. Am. Ceram. Soc.*, 1999, **82**(5), 1229–1232.
7. Hannink, R. H. J., Kelly, P. M. and Muddle, B. C., Transformation toughening in zirconia-containing ceramics. *J. Am. Ceram. Soc.*, 2000, **83**(3), 461–487.
8. Casellas, D., Nagl, M. M., Llanes, L. and Anglada, M., Fracture toughness of alumina and ZTA ceramics: micro-structural coarsening effects. *J. Mater. Process. Tech.*, 2003, **143–144**, 148–152.
9. Janney, M. A., Nunn, S. D., Walls, C. A., Omatete, O. O., Ogle, R. B., Kirby, G. H. *et al.*, Gelcasting. In *The Handbook of Ceramic Engineering*, ed. M. N. Rahman. Marcel Dekker, New York, 1998, pp. 1–15.
10. Tari, G., Gelcasting ceramics: a review. *Am. Ceram. Soc. Bull.*, 2003, **82**(4), 42–46, and references therein.
11. Kosmac, T., Novak, S. and Sajko, M., Hydrolysis-assisted solidification (HAS): a new setting concept for ceramic net-shaping. *J. Eur. Ceram. Soc.*, 1997, **17**, 427–432.
12. Ganesh, I., Thiyagarajan, N., Jana, D. C., Barik, P., Sundararajan, G. and Ferreira, J. M. F., Dense β-SiAlONs consolidated by a modified hydrolysis assisted solidification route. *J. Eur. Ceram. Soc.*, 2008, **28**(4), 879–885.
13. Ganesh, I., Thiyagarajan, N., Jana, D. C., Barik, P. and Sundararajan, G., An aqueous gelcasting route to dense β-$Si_4Al_2O_2N_6$–0.5SiO_2 ceramics. *J. Am. Ceram. Soc.*, 2008, **91**(5), 1566–1571.
14. Ganesh, I., Jana, D. C., Shaik, S. and Thiyagarajan, N., An aqueous gelcasting process for sintered silicon carbide ceramics. *J. Am. Ceram. Soc.*, 2006, **89**(10), 3056–3064.
15. Kirby, K. W., Jankiewicz, A. T., Lowell, R. F., and Hallse, R. L., Near net shape fabrication of ceramic radomes. US Patent 6,083,452 (July 4, 2000).
16. Ganesh, I., Near-net shape β-$Si_4Al_2O_2N_6$ parts by hydrolysis induced aqueous gelcasting process. *Int. J. Appl. Ceram. Technol.*, 2008, **6**, 89–101.
17. Ganesh, I., Teja, K. A., Thiyagarajan, N., Johnson, R. and Reddy, B. M., Formation and densification behaviour of magnesium aluminate spinel: the influence of CaO and moisture in the precursors. *J. Am. Ceram. Soc.*, 2005, **88**(10), 2752–2761.
18. Cullity, B. D., *Elements of XRD* (*2nd ed.*). Addison-Wesley, Reading, MA, 1978.
19. Klug, M. P. and Alexander, L. E., *X-ray Diffraction Procedure for Polycrystalline and Amorphous Materials*. Wiley, New York, 1974, p. 634.
20. Anstis, G. R., Chantikul, P., Lawn, B. R. and Marshall, D. B., A critical evaluation of indentation techniques for measuring fracture toughness. I. Direct crack measurements. *J. Am. Ceram. Soc.*, 1981, **64**, 533–538.
21. Olhero, S. M., Tari, G., Coimbra, M. A. and Ferreira, J. M. F., Synergy of polysaccharide mixtures in gelcasting of alumina. *J. Eur. Ceram. Soc.*, 2000, **20**, 423–429.
22. Novak, S., Kosmac, T., Krnel, K. and Draz, G., Principles of the hydrolysis assisted solidification (HAS) process for forming ceramic bodies from aqueous suspension. *J. Eur. Ceram. Soc.*, 2002, **22**, 289–295.
23. Krnel, K. and Kosmac, T., Protection of AlN powder against hydrolysis using aluminum di-hydrogen phosphate. *J. Eur. Ceram. Soc.*, 2001, **21**, 2075–2079.
24. Janney, M. A., Walls, C. A., Kupp, D. M. and Kirby, K. W., Gelcasting SiAlON radomes. *Am. Ceram. Soc. Bull.*, 2004, 9201–9206.
25. Deville, S., Chevalier, J., Fantozzi, G., Bartolome, J. F., Requena, J., Moya, J. S. *et al.*, Low-temperature ageing of zirconia-toughened alumina ceramics and its implication in biomedical implants. *J. Eur. Ceram. Soc.*, 2003, **23**, 2975–2982.